Online compressed sening MR image reconstruction for high resolution T_2* imaging

L. El Gueddari [1,2], P. Ciuciu[1,2], E. Chouzenoux [3,4], A. Vignaud [1] and J-C. Pesquet[3]

[1]CEA/NeuroSpin, Gif-sur-Yvette, France [2]INRIA-CEA Saclay Ile-de-France, Parietal team, Univ Paris-Saclay, France [3]CVN, Centrale-Supélec, Univ. Paris-Saclay, France [4]LIGM, Paris-Est University, France

ISMRM 2019, Montreal, Canada

Outline

1. Compressed Sensing in MRI
   - Faster acquisition for high-resolution MRI
   - Compressed sensing in MRI
2. Online reconstruction
   - Problem statement
   - Optimization algorithm
3. Experiments: General setting
4. Cartesian under-sampling: Experiments & Results
   - Cartesian setting
   - Cartesian results
5. Non-Cartesian under-sampling: Experiments & Results
   - Non-Cartesian setting
   - Non-Cartesian results

Context

High resolution MRI:

- improves the spatial definition $\rightarrow$ helps early diagnosis
- requires longer acquisition time

[1] Griswold et al. 2002, *Magnetic Resonance in Medicine.*
[2] Pruessmann et al. 1999, *Magnetic Resonance in Medicine*.
[3] Feinberg et al. 1986, *Radiology*.
[4] Hargreaves et al. 2004, *Magnetic Resonance in Medicine*.
[5] Lustig, Donoho, and Pauly 2007, *Magnetic Resonance in Medicine*.
[6] Lazarus et al. 2019, *Magnetic Resonance in Medicine*.

Context

High resolution MRI:

- improves the spatial definition $\rightarrow$ helps early diagnosis
- requires longer acquisition time

To reduce this acquisition time many methods have been proposed:

[1] Griswold et al. 2002, *Magnetic Resonance in Medicine.*
[2] Pruessmann et al. 1999, *Magnetic Resonance in Medicine*.
[3] Feinberg et al. 1986, *Radiology*.
[4] Hargreaves et al. 2004, *Magnetic Resonance in Medicine*.
[5] Lustig, Donoho, and Pauly 2007, *Magnetic Resonance in Medicine*.
[6] Lazarus et al. 2019, *Magnetic Resonance in Medicine*.

Context

High resolution MRI:

- improves the spatial definition → helps early diagnosis
- requires longer acquisition time

To reduce this acquisition time many methods have been proposed:

- Parallel MRI[1,2]

[1] Griswold et al. 2002, *Magnetic Resonance in Medicine.*
[2] Pruessmann et al. 1999, *Magnetic Resonance in Medicine*.
[3] Feinberg et al. 1986, *Radiology*.
[4] Hargreaves et al. 2004, *Magnetic Resonance in Medicine*.
[5] Lustig, Donoho, and Pauly 2007, *Magnetic Resonance in Medicine*.
[6] Lazarus et al. 2019, *Magnetic Resonance in Medicine*.

Context

High resolution MRI:

- improves the spatial definition $\rightarrow$ helps early diagnosis
- requires longer acquisition time

To reduce this acquisition time many methods have been proposed:

- Parallel MRI[1,2]
- Partial Fourier[3]

[1] Griswold et al. 2002, *Magnetic Resonance in Medicine.*
[2] Pruessmann et al. 1999, *Magnetic Resonance in Medicine.*
[3] Feinberg et al. 1986, *Radiology.*
[4] Hargreaves et al. 2004, *Magnetic Resonance in Medicine.*
[5] Lustig, Donoho, and Pauly 2007, *Magnetic Resonance in Medicine.*
[6] Lazarus et al. 2019, *Magnetic Resonance in Medicine.*

Context

High resolution MRI:

- improves the spatial definition → helps early diagnosis
- requires longer acquisition time

To reduce this acquisition time many methods have been proposed:

- Parallel MRI[1,2]
- Partial Fourier[3]
- Simultaneous Multi-Slice[4]

---

[1] Griswold et al. 2002, *Magnetic Resonance in Medicine.*
[2] Pruessmann et al. 1999, *Magnetic Resonance in Medicine.*
[3] Feinberg et al. 1986, *Radiology.*
[4] Hargreaves et al. 2004, *Magnetic Resonance in Medicine.*
[5] Lustig, Donoho, and Pauly 2007, *Magnetic Resonance in Medicine.*
[6] Lazarus et al. 2019, *Magnetic Resonance in Medicine.*

Context

High resolution MRI:

- improves the spatial definition $\rightarrow$ helps early diagnosis
- requires longer acquisition time

To reduce this acquisition time many methods have been proposed:

- Parallel MRI[1,2]
- Partial Fourier[3]
- Simultaneous Multi-Slice[4]
- Compressed Sensing[5]

---

[1] Griswold et al. 2002, *Magnetic Resonance in Medicine.*
[2] Pruessmann et al. 1999, *Magnetic Resonance in Medicine.*
[3] Feinberg et al. 1986, *Radiology.*
[4] Hargreaves et al. 2004, *Magnetic Resonance in Medicine.*
[5] Lustig, Donoho, and Pauly 2007, *Magnetic Resonance in Medicine.*
[6] Lazarus et al. 2019, *Magnetic Resonance in Medicine.*

Context

High resolution MRI:

- improves the spatial definition $\rightarrow$ helps early diagnosis
- requires longer acquisition time

To reduce this acquisition time many methods have been proposed:

- Parallel MRI[1,2]
- Partial Fourier[3]
- Simultaneous Multi-Slice[4]
- Compressed Sensing[5] $\leftarrow$ reaches higher acceleration factors[6]

---

[1] Griswold et al. 2002, *Magnetic Resonance in Medicine.*
[2] Pruessmann et al. 1999, *Magnetic Resonance in Medicine.*
[3] Feinberg et al. 1986, *Radiology.*
[4] Hargreaves et al. 2004, *Magnetic Resonance in Medicine.*
[5] Lustig, Donoho, and Pauly 2007, *Magnetic Resonance in Medicine.*
[6] Lazarus et al. 2019, *Magnetic Resonance in Medicine.*

Context

High resolution MRI:

- improves the spatial definition → helps early diagnosis
- requires longer acquisition time

To reduce this acquisition time many methods have been proposed:

- Parallel MRI[1,2]
- Partial Fourier[3]
- Simultaneous Multi-Slice[4]
- Compressed Sensing[5] ← reaches higher acceleration factors[6]

[1] Griswold et al. 2002, *Magnetic Resonance in Medicine.*
[2] Pruessmann et al. 1999, *Magnetic Resonance in Medicine.*
[3] Feinberg et al. 1986, *Radiology*.
[4] Hargreaves et al. 2004, *Magnetic Resonance in Medicine*.
[5] Lustig, Donoho, and Pauly 2007, *Magnetic Resonance in Medicine*.
[6] Lazarus et al. 2019, *Magnetic Resonance in Medicine*.

Compressed Sensing MRI

Provides theoretical guarantees of exact reconstruction under three main pillars:

- Sparse decomposition in a dictionary (Wavelet, Total Variation, Frames, ...)

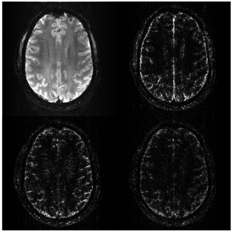

Figure: Sparse decomposition using wavelet basis

Compressed Sensing MRI

Provides theoretical guarantees of exact reconstruction under three main pillars:

- Sparse decomposition in a dictionary (Wavelet, Total Variation, Frames, ...)
- Asymptotically incoherent acquisition with respect to this sparse decomposition[7]

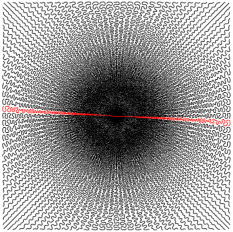

Figure: Under sampled K-space used to accelerate the acquisition

Compressed Sensing MRI

Provides theoretical guarantees of exact reconstruction under three main pillars:

- Sparse decomposition in a dictionary (Wavelet, Total Variation, Frames, ...)
- Asymptotically incoherent acquisition with respect to this sparse decomposition[7]
- Reconstruction that promotes the sparsity.

$$\hat{\boldsymbol{x}} = \underset{\boldsymbol{x} \in \mathbb{C}^N}{\operatorname{argmin}} \frac{1}{2} \|\boldsymbol{y} - F_\Omega \boldsymbol{x}\|_2^2 + \lambda \|\boldsymbol{\Psi} \boldsymbol{x}\|_1$$

with:

- $\boldsymbol{\Psi}$: sparse decomposition
- $\boldsymbol{x}$: MR image to be recovered
- $\boldsymbol{y}$: under-sampled k-space data
- F_Ω: under-sampled Fourier operator on the support Ω
- $\lambda > 0$: hyper-parameter

[7] Adcock et al. 2017.

Compressed sensing limitations

Reconstruction time is long especially for:

- Highly accelerated acquisition with non-Cartesian sampling schemes
- when nonuniform Fourier transform[8,9] is needed

Our proposition:

- Start the reconstruction from incomplete data
- Interleave acquisition and reconstruction

This will allow us to give a continuous feedback to the radiologist along the scan.

[8] Fessler and Sutton 2003, *IEEE Transactions on Signal Processing*.

[9] Keiner, Kunis, and Potts 2009, *ACM Transactions on Mathematical Software (TOMS)*.

Our approach for online MR image reconstruction

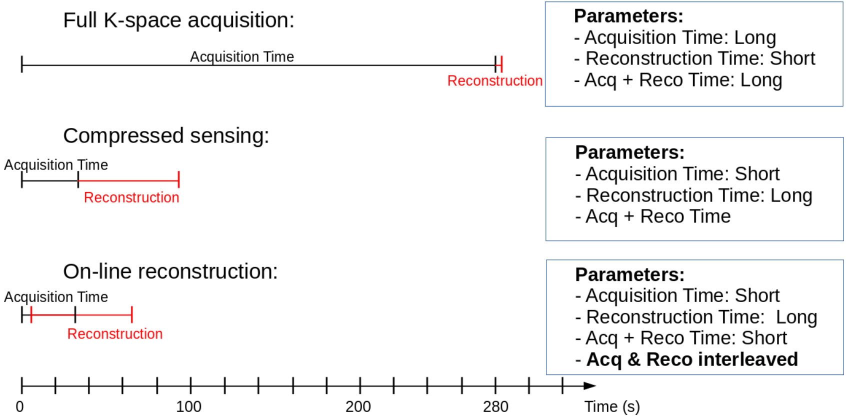

Figure: *Online* MR image reconstruction framework

Online reconstruction: Problem statement

Online MR image reconstruction is formulated as follows:

$$\forall j \in \mathbb{N}, 0 < j \leqslant n_b; \quad \hat{\boldsymbol{x}}^j = \underset{\boldsymbol{x} \in \mathbb{C}^N}{\operatorname{argmin}} \frac{1}{2\#\Omega_j} \left\{ \| F_{\Omega_j} \boldsymbol{x} - \boldsymbol{y} \|_2^2 + \lambda \| \boldsymbol{\Psi} \boldsymbol{x} \|_1 \right\}$$

With:

- n_b: the number of batches
- s_b: the number of spokes in a batch
- n_j: the number of iterations in each batch
- Γ_i: the support of the i^{th} shot
- $\Omega_j = \bigcup_{0 \leqslant i \leqslant j\, s_b} \Gamma_i$ is the *cumulative* set of the $j\, s_b$ collected spokes

Online reconstruction: Problem statement

Online MR image reconstruction is formulated as follows:

$$\forall j \in \mathbb{N}, 0 < j \leqslant n_b; \quad \hat{\boldsymbol{x}}^j = \underset{\boldsymbol{x} \in \mathbb{C}^N}{\operatorname{argmin}} \frac{1}{2\#\Omega_j} \left\{ \| F_{\Omega_j} \boldsymbol{x} - \boldsymbol{y} \|_2^2 + \lambda \| \boldsymbol{\Psi} \boldsymbol{x} \|_1 \right\}$$

With:

- n_b: the number of batches
- s_b: the number of spokes in a batch
- n_j: the number of iterations in each batch
- Γ_i: the support of the i^{th} shot
- $\Omega_j = \bigcup_{0 \leqslant i \leqslant j\, s_b} \Gamma_i$ is the *cumulative* set of the $j\, s_b$ collected spokes

At the end of the acquisition the online and offline problems are equivalent.

We aim to find:

$$\underline{\widehat{\boldsymbol{x}}} \in \underset{\boldsymbol{x} \in \mathbb{C}^N}{\arg\min} \left[f(\boldsymbol{x}) + g(\boldsymbol{\Psi x}) \right] \tag{1}$$

where:

- f is convex, differentiable on $\mathbb{C}^N$ and its gradient is β-Lipschitz
- $g \in \Gamma_0(\mathbb{C}^{N_\Psi})$ with a closed form proximity operator, given by:

$$\text{prox}_g(\boldsymbol{z}) = \underset{\boldsymbol{v} \in \mathbb{C}^{N_\Psi}}{\arg\min} \frac{1}{2} \|\boldsymbol{z} - \boldsymbol{v}\|^2 + g(\boldsymbol{v}) \tag{2}$$

Note: Those are standard assumptions in optimization-based image reconstruction methods.
The problem is convex (i.e. does not depends on the initialization)

Condat-Vũ Algorithm

We adapted and implemented Condat[10]-Vũ[11] algorithm as follows:

Algorithm 1: Condat-Vú algorithm

initialize $i = 1, j = 1, \boldsymbol{x}_1^1, \boldsymbol{z}_1^1$;
while $j \leq n_b$ **do**
  $\kappa_j := \frac{\beta_j}{2\|\boldsymbol{T}\|^2}$;
  $\tau_j := \frac{1}{\beta_j}$;
  while $i \leq n_j$ **do**
    $\boldsymbol{x}_{i+1}^j := \boldsymbol{x}_i^j - \tau_j \left(\nabla f_{\Omega_j}(\boldsymbol{x}_i^j) + \boldsymbol{T}^* \boldsymbol{z}_i^j\right)$;
    $\boldsymbol{w}_{i+1}^j := \boldsymbol{z}_i^j + \kappa_j \boldsymbol{T} \left(2\boldsymbol{x}_{i+1}^j - \boldsymbol{x}_i^j\right)$;
    $\boldsymbol{z}_{i+1}^j := \boldsymbol{w}_{i+1}^j - \kappa_j \operatorname{prox}_{g/\kappa_j}\left(\frac{\boldsymbol{w}_{i+1}^j}{\kappa_j}\right)$;
    $i := i + 1$;
  end
  $\boldsymbol{x}_1^{j+1} := \boldsymbol{x}_{n_k}^j$;
  $\boldsymbol{z}_1^{j+1} := \boldsymbol{z}_{n_k}^j$;
  $j := j + 1$;
end

Figure: Optimization algorithm

with:

- $\boldsymbol{z} = \boldsymbol{\Psi x}$
- β_j the Lipschitz constant of the spectral norm of f_{Ω_j}

[10] Condat 2013, *Journal of Optimization Theory and Applications*.
[11] Vũ 2013, *Advances in Computational Mathematics*.

Experiments parameters

Acquisition parameters:

- T2*-weighted ex-vivo baboon brain
- scanned at 7T
- Resolution: $0.4 \times 0.4 \times 3\text{mm}^3$
- FOV: 20.4cm
- Base resolution: 512×512
- TR: 550 ms (11 slices)
- TE: 30 ms
- FA: 25°

Reconstruction parameters:

- decimated Bi-Orthogonal 7/9 Wavelet transform
- Hyper-parameter λ was set retrospectively
- Final number of iterations was set to 200
- Open source code available on `PySAP`
- 128 GB of RAM and an 8-core (2.40 GHz) Intel Xeon E5-2630 v3 Processor

Retrospective Cartesian under-sampling

Parameter setting

- Sampling mask: 187 lines of 512 samples each
- Under-sampling factor: 2.7
- 12 central lines were acquired first and the others in pseudo random order next
- FFT was used
- Time per iteration $T_{it} = 0.12$s

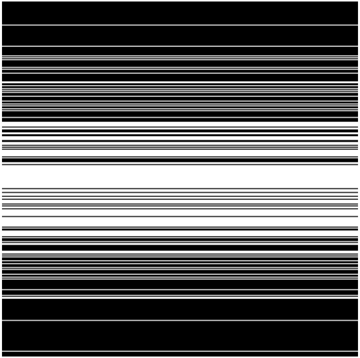

Figure: Retrospective under-sampling Cartesian mask.

Retrospective Cartesian acquisition

Batch setup

Table: Parameter setting for Cartesian acquisitions.

	Batch size s_b	Iterations n_j
$s_b = 2$	[2, 4, 6, ...,182, 184, 187]	[9, 9, 9, ..., 9, 200]
$s_b = 23$	[23, 46, 69, 92, 115, 138, 161, 187]	[100, 100, ..., 100, 200]
$s_b = 46$	[46, 92, 138, 187]	[200, 200, 200, 200]
$s_b = 92$	[92, 187]	[400, 200]
Offline	[187]	[200]

Results: SSIM[12] scores

Cartesian under-sampling

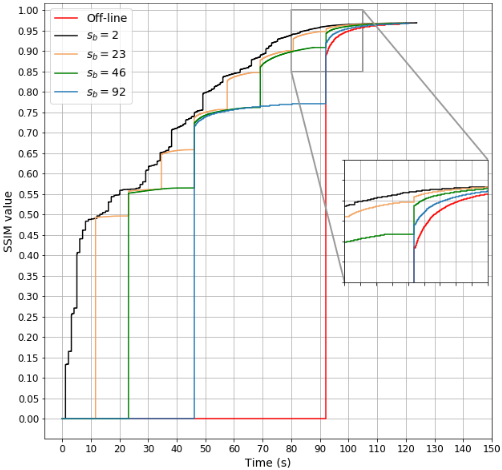

Figure: Comparison of SSIM scores for different batch sizes.

[12] Wang et al. 2004, *IEEE Transactions on Image Processing*.

Results: Images by the end of the acquisition

Cartesian under-sampling

Cartesian Reference	$s_b = 2$ SSIM$= 0.961$	$s_b = 23$ SSIM$= 0.948$	$s_b = 46$ SSIM$= 0.909$	$s_b = 96$ SSIM$= 0.772$

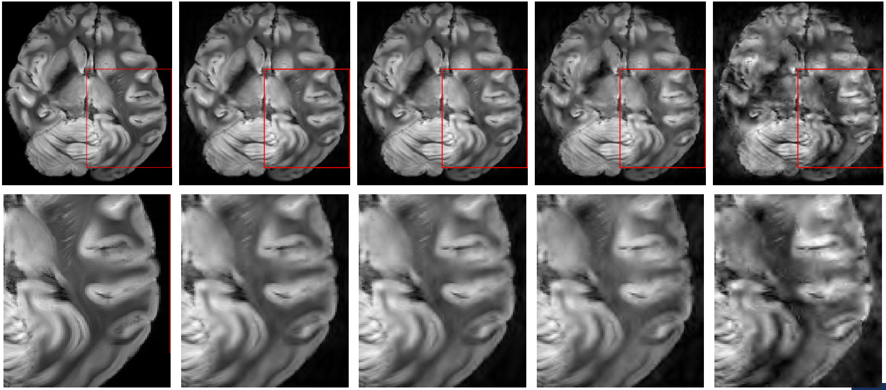

Figure: MR images delivered by the end of acquisition.

Prospective non-Cartesian under-sampling

Parameter setting

A modified T2* weighted GRE sequence was implemented based on the multi-shot Sparkling[a] trajectories:

- Number of shots: 43
- Number of samples per shots: 3072
- Acceleration factor: 12 in time
- Under-sampling factor: 2
- Sequence was implemented using a golden angle approach ($\approx 112^\circ$ between consecutive shots)
- NFFT[b] was used
- Time per iteration: 0.25s

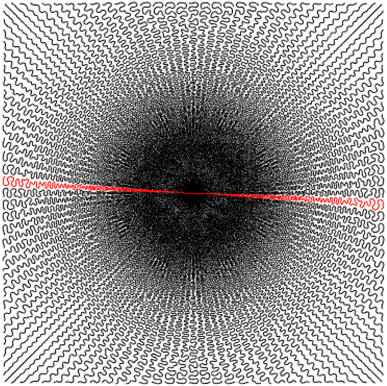

Figure: Prospective Sparkling under-sampling scheme.

[a] Lazarus et al. 2019, *Magnetic Resonance in Medicine*.

[b] Keiner, Kunis, and Potts 2009, *ACM Transactions on Mathematical Software (TOMS)*.

Prospective non-Cartesian acquisition

Batch setup

Table: Parameter setting for non-Cartesian acquisitions.

	Batch size s_b	Iterations n_j
Offline	[43]	[200]
H_1	[5, 15, 29, 43]	[22, 30, 30, 200]
H_2	[7, 14, 21, 28, 35, 43]	[15, 15, 15, 15, 17, 200]
H_3	[4, 8, 12, 16, ..., 40, 43]	[8, 8, 8, ..., 8, 6, 200]

Results: SSIM scores

Non-Cartesian under-sampling

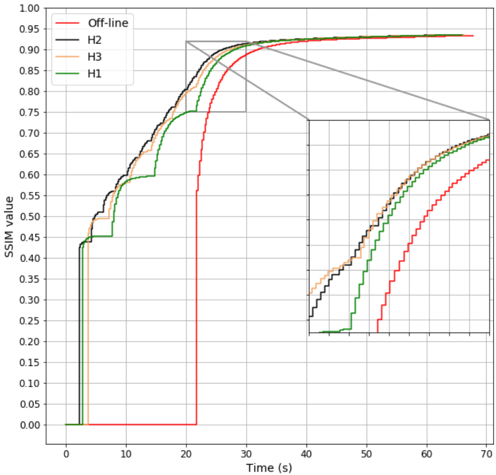

Figure: Comparison of SSIM scores for different batch setups.

Results: Images by the end of the acquisition

Non-Cartesian under-sampling

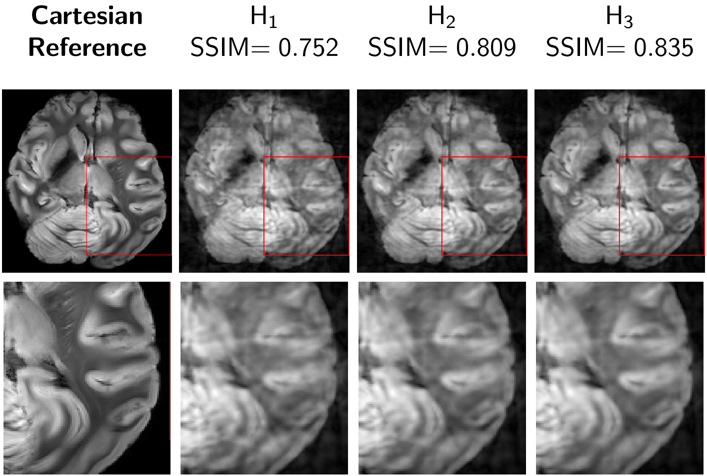

Figure: MR images delivered by the end of acquisition.

Conclusions & Outlook

Conclusions:

- We proposed a new image reconstruction framework that takes the sequential structure of multi-shot MR acquisition into account.
- This methods provides an online feedback during MR acquisition.
- Compared to offline CS reconstruction, our approach is able to provide online feedback by the end of MR acquisition, both for Cartesian and non-Cartesian sampling.
- We compared multiple batch sizes to get the best reconstruction by the end of the acquisition $\rightarrow$ small batch sizes give improved results.
- In the given allocated acquisition time, our approach achieves better image quality for Cartesian under-sampling as the time per iteration is cheaper.

Perspectives:

- Extension to the multi-channel acquisition (calibration-less, beyond ℓ_1-norm regularization)
- Integration in the Gadgetron framework to enable this feedback directly on the scanner.

Acknowledgements

This project has been granted by the mobility grant of the SFRMBM and the FLI society

ISMRM ONE
COMMUNITY FOR CLINICIANS AND SCIENTISTS

FLi
France Life Imaging

SFRMBM
SOCIÉTÉ FRANÇAISE DE RÉSONANCE MAGNÉTIQUE EN BIOLOGIE & MÉDECINE

References I

Adcock, B. et al. (2017). "Breaking the coherence barrier: A new theory for compressed sensing". In: *Forum of Mathematics, Sigma*. Vol. 5. Cambridge University Press.

Condat, L. (2013). "A primal–dual splitting method for convex optimization involving Lipschitzian, proximable and linear composite terms". In: *Journal of Optimization Theory and Applications* 158.2, pp. 460–479.

Feinberg, David A et al. (1986). "Halving MR imaging time by conjugation: demonstration at 3.5 kG.". In: *Radiology* 161.2, pp. 527–531.

Fessler, J.A. and B.P. Sutton (2003). "Nonuniform fast Fourier transforms using min-max interpolation". In: *IEEE Transactions on Signal Processing* 51.2, pp. 560–574.

Griswold, Mark A et al. (2002). "Generalized autocalibrating partially parallel acquisitions (GRAPPA)". In: *Magnetic Resonance in Medicine.* 47.6, pp. 1202–1210.

Hargreaves, Brian A et al. (2004). "Variable-rate selective excitation for rapid MRI sequences". In: *Magnetic Resonance in Medicine* 52.3, pp. 590–597.

References II

Keiner, J., S. Kunis, and D. Potts (2009). "Using NFFT 3—a software library for various nonequispaced fast Fourier transforms". In: *ACM Transactions on Mathematical Software (TOMS)* 36.4, p. 19.

Lazarus, Carole et al. (2019). "SPARKLING: variable-density k-space filling curves for accelerated T2*-weighted MRI". In: *Magnetic Resonance in Medicine* 81.6, pp. 3643–3661.

Lustig, M., D.L. Donoho, and J.M. Pauly (2007). "Sparse MRI: The application of compressed sensing for rapid MR imaging". In: *Magnetic Resonance in Medicine* 58.6, pp. 1182–1195.

Pruessmann, K.P. et al. (1999). "SENSE: sensitivity encoding for fast MRI". In: *Magnetic Resonance in Medicine* 42.5, pp. 952–962.

Vũ, BC (2013). "A splitting algorithm for dual monotone inclusions involving cocoercive operators". In: *Advances in Computational Mathematics* 38.3, pp. 667–681.

Wang, Zhou et al. (2004). "Image quality assessment: from error visibility to structural similarity". In: *IEEE Transactions on Image Processing* 13.4, pp. 600–612.